Suspension system of the Barrel Toroid cold mass

C. Mayri, C. Berriaud, S. Cazaux, A. Dudarev, A. Foussat, Y. Pabot, JM Rey, M. Reytier, H. ten Kate, Z. Sun, P. Védrine, Y. Zaitsev

Abstract— The ATLAS Barrel Toroid consists of 8 racetrack coils symmetrically placed around the LHC beam axis. The coil dimensions are 25-m of length, 5-m of width and 1-m of thickness. Each cold mass is held in its cryostat by different types of supports. The paper describes the design, the tests and the behaviour of each element during on surface test of individual coils.

Index Terms— Cryogenic stop, friction, sliding system, tie rod.

I. INTRODUCTION

The eight coils of the ATLAS Barrel Toroid magnet [1] are submitted to the gravity in different direction according to their location in the toroid, to the thermal shrinkage during the cool down or the warm up and to the magnetic centripetal forces once the magnet is energized. Cold mass suspension system (Fig. 1 and 2) consists of two main components: the tie rods which have to take the magnetic force of 1500 tons and accommodate the thermal shrinkage of 45-mm at each extremity, and the cryogenic stops which are supporting the cold mass weight of 45 tons and also putting up with the thermal shrinkage. The tie rods are made in titanium alloy and take the thermal shrinkage by flexion. The cryogenic stops are made in epoxy resin-glass fibre composite and allow the displacement of the cold mass relatively to the vacuum vessel by a dedicated sliding system. Each of them was designed to support the mechanical loading and to minimize the thermal loads. Prior to their installation, some elements were tested individually on dedicated test bench. The final production was tested in real conditions during the on surface test. A G11 bar in the middle of the coil fixes longitudinally the cold mass.

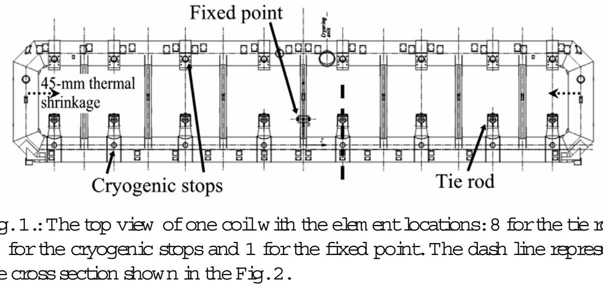

Fig. 1.: The top view of one coil with the element locations: 8 for the tie rods, 16 for the cryogenic stops and 1 for the fixed point. The dash line represents the cross section shown in the Fig. 2.

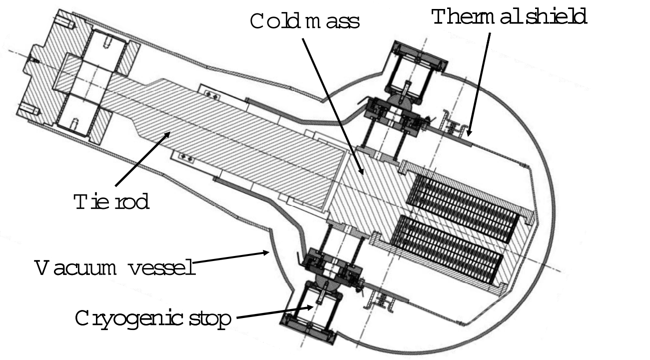

Fig. 2.: Coil section oriented at 22.5° as in one of the inclinations in the final toroid assembly.

II. TIE ROD COMPONENT

Each cold mass is supported inside the vacuum vessel by 8 tie rods shared on the two sides of the magnet (side A and C) and designed to withstand the radial magnetic forces (about 200 tons on each) and to accommodate the relative longitudinal displacement of the cold mass with respect to the vacuum vessel during the cooling down (about 45 mm on the outermost tie rod). At the operating conditions the head of the tie rod is near the room temperature whereas the foot is about at 10 K. The middle of the tie rod is thermally connected to the thermal shield at about 80K to minimize the heat load on the cold mass. In order to do that the Ti5Al2.5 Sn ELI (Extra Low Interstitial) grade titanium alloy is used for the manufacturing (Fig. 3) which is done in Russia under the supervision of the Lutch Institute.

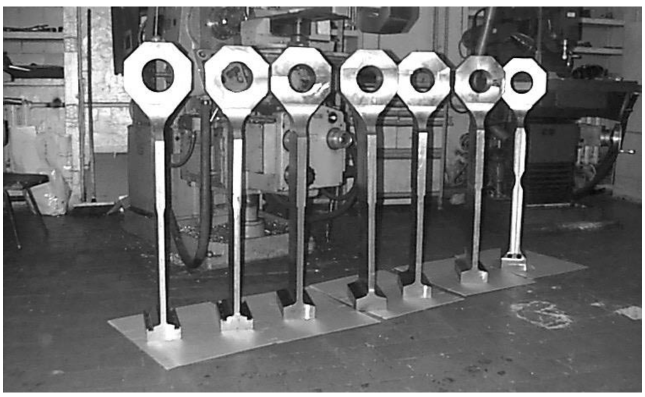

Fig. 3.: Tie rods after machining.

Manuscript received September 19, 2005.
C.M., C.B., S.C., Y.P., JM R., M.R., Z.S. and P.V. are is with CEA DSM/DAPNIA, 91191 Gif-sur-Yvette Cedex
A.D., A.F., H.t.K. and Y.Z. are with CERN, 1211 Geneva 23

A. Design

The allowable stress limits (410 MPa in the warm part of the tie rod and 670 MPa in its cold part) are strictly respected in the design (Fig. 4). Due the temperature, the foot is mainly concerned by the brittle rupture. Extensive campaigns of measurements of the mechanical and physical properties, as ultrasonic controls, have been done in order to asses the quality of the material.

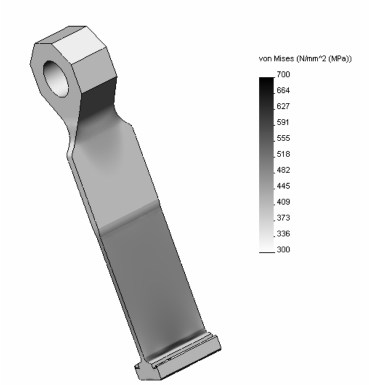

Fig. 4.: A tie rod computation by finite element analysis gives a cold web stress around 500 MPa with very small zones at 650 MPa in the foot.

B. Individual cold tests

After the final machining, all the 64 tie rods have been proof tested at 4.2 K by the Kurchatov Institute (Moscow) up to a 250 ton load in a special cryostat (Fig. 6) which allows testing two tie rods at the same time [2]. Four hydraulic jacks are pulling the tie rod heads whereas their feet are cooled by a circulation of liquid helium in copper tubes in good thermal contact with the foot support piece. A vacuum vessel surrounds a nitrogen shield and the assembly. Typical test diagram showing the force to overall elongation is shown the Figure 5. The elongation shown in the figure is the overall elongation of the tie rod including the cryostat parts. The tie rod elongation itself has been measured to 1.6 mm for a 250 ton load. All the tie rods have successfully passed the proof load tests.

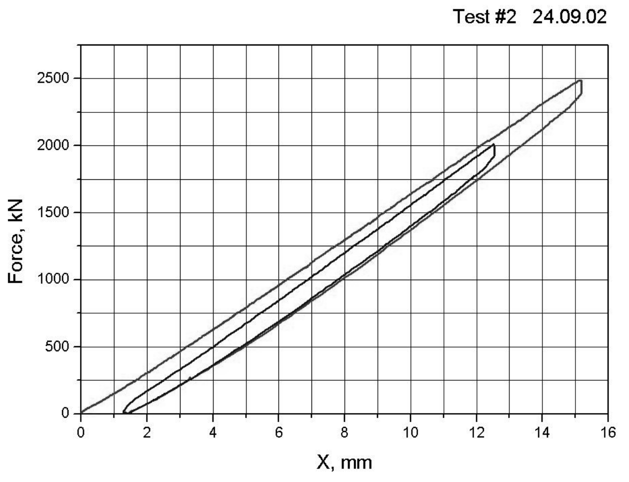

Fig. 5.: Elongation diagram during the proof test of a tie rod couple.

Fig. 6.: Test bench of the tie rods at cryogenic temperature.

C. Behavior during coil test

All the 8 individual coils have been cold tested in a special test station on surface before to be installed in the cavern [3,4]. A magnetic mirror is installed near the coil to reproduce the attractive magnetic force seen by the coils in the cavern with the toroidal configuration. During these tests, the eight tie-rods have been equipped with strain gauges on both sides to measure both the elongation and the bending of the tie-rods. The strain gauges are mounted in full bridge configuration in order to compensate for temperature changes and magnetic field. The two outermost tie-rods (3 & 4) are equipped with a double set of gages. In order to minimize the strain in the tie rods when the coil is at its operating temperature, the tie-rods are mounted with a bending, such that a stress-free state at operating temperature should be reached before to energize the coil.

When the coil is powered, the attractive force between the coil and the magnetic mirror is transferred to the tie-rods. The load on the tie-rods in the test station is comparable to the load in the final toroidal configuration in the cavern. Of course there is also a bending force on the tie-rods when the coil is powered because the coil elongates by about 3 mm. This resulting bending stresses are much smaller than the axial loading.

The measured displacements of the tie-rods during the cooling down are in agreement with the calculations as shown in the Table 1.

Displacement (mm)	Tie-rod 4	Tie-rod 3	Tie-rod 2	Tie-rod 1
Calculated	45	34.2	21.3	7
Measured	45	33	20	6

TABLE 1: CALCULATED AND MEASURED DISPLACEMENTS OF THE TIE-RODS DURING THERMAL CYCLING.

The elongation of the tie-rods is quite linear with the square of the current and shows no hysteresis when ramped down (Fig.7). The sharing of the forces between each tie-rod (Table 2) is done as expected, but with maximum forces at roughly 80% of those calculated. This difference may come from the modeling of the iron wall effect.

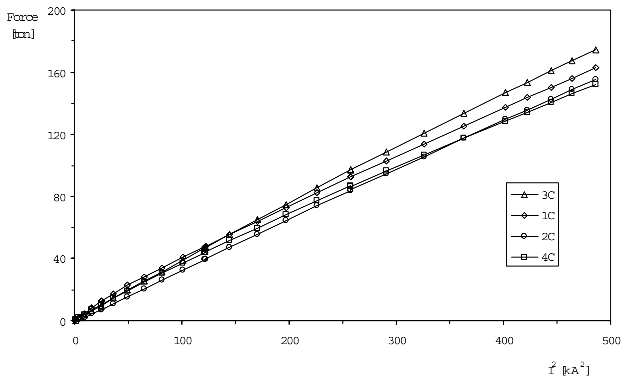

Fig.7.: Evolution of the force in the tie rods with the square of the current.

Tie-rod #	4A	3A	2A	1A	1C	2C	3C	4C
Measured load, [ton]	150	175	160	152	163	155	174	152
Calculated load [ton]	184	212	190	195	195	190	212	184

TABLE 2: MEASURED AND CALCULATED LOAD ON THE TIE-RODS AT 22 KA.

III. CRYOGENIC STOPS

The stops are split in two parts: a cold post between 5 K and 60 K on which the thermal shields are fixed and a warm post between 60 K and 300 K. A sliding system between them, based on a deposition of Nuflon-N™ from the APS Company (France), allows the coil movement during the thermal phases. Figure 9 shows a whole stop built by Hoch Technologie Systeme in Switzerland.

A. Design

Each post is a stratified composite tube glued in two end flanges. The tube is a mixture of epoxy resin and glass fiber. The volume fiber content is about 55%. The mechanical behavior, mainly given by the winding angle of the fibers and the tube thickness, was studied in details in order to support the thermal shrinkage of this piece, which induces very high stresses between the layers, and the mechanical loads of compression and flexion. This study took in consideration the different running phase: the loading at warm temperature, the cooling down (or warming up) which generates the sliding of the coil on the warm posts and the coil quench which creates additional forces on the cold posts. The hypotheses are an axial loading of 6 tons with a friction coefficient of 0.2 on the sliding system. In our case, the optimal winding angle is very high: ±75° in relation to the tube axis, with a tube thickness of 10 mm. This design gives a safety factor of 2 on the first ply failure according to Tsai-Hill criteria.

We also studied very carefully the gluing of the post in their end flanges (Fig.8), because the thermal contraction creates in this area a dangerous shear stress. It led to a specific profile of the flange in order to limit the peak of shear stress.

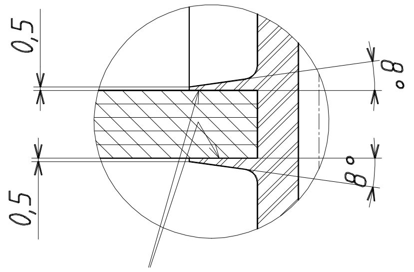

Fig.8.: The design of the gluing groove, based on the thin conical part of the flange, creates a very efficient decrease of the shear stress.

B. Individual cold test

We built specific equipment (Fig. 9) in order to test a complete stop (the two posts and the sliding system) in cryogenic conditions. In order to create an axial thermal gradient in the posts, the sliding system is cooled down at 80 K whereas the ends of the stop stay at room temperature. After applying 40 kN axially, a jack creates an alternative transverse cycling on a 45 mm stroke at 1 mm/min to simulate the sliding during the cool down or the warm up of the coil. The strain gauges glued on each face of the posts give indirectly the deformations due to the axial forces or to the transversal forces. Then we can survey the post behavior and compute the friction coefficient of the sliding system (Fig.10 and 11).

The experimental equivalent axial E-modulus is 14 GPa instead of the 11 GPa found in the computation. It brings to light the difficulty to compute the properties of such material.

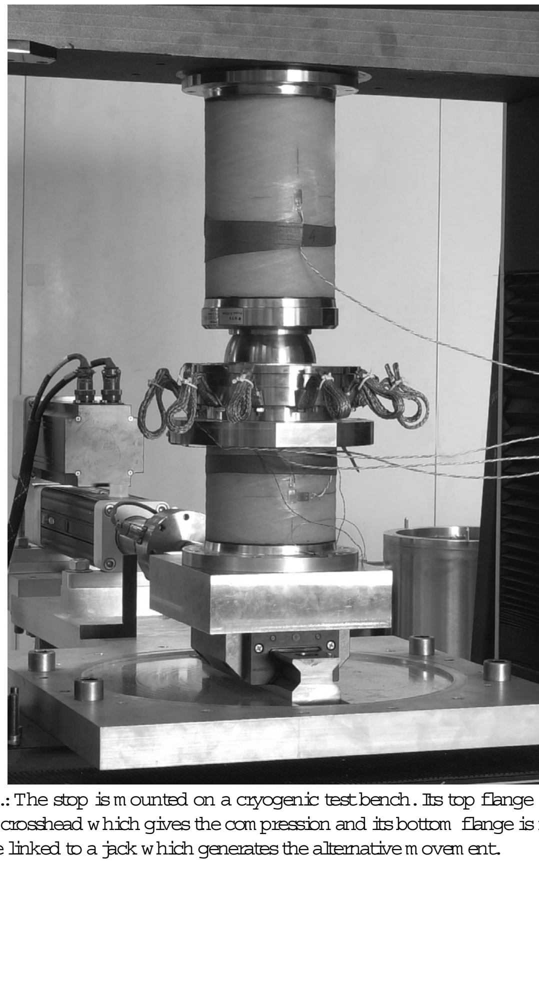

Fig.9.: The stop is mounted on a cryogenic test bench. Its top flange is fixed to the crosshead which gives the compression and its bottom flange is fixed to a table linked to a jack which generates the alternative movement.

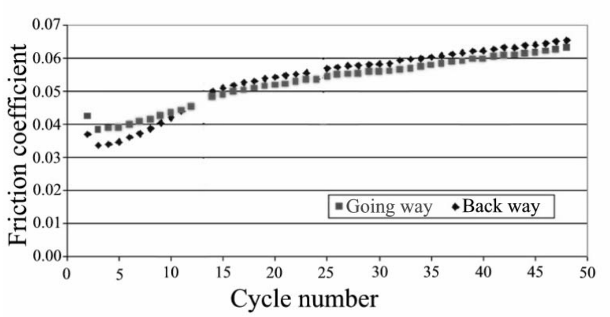

Fig. 10.: Friction coefficient against cycle numbers at 300 K under atmospheric pressure.

As shown on the graph in the Figure 10, the increase of the friction coefficient with the number of cycles is obvious, but it appears only at room conditions. Under vacuum or at cryogenic temperature, the coefficient is quite constant.

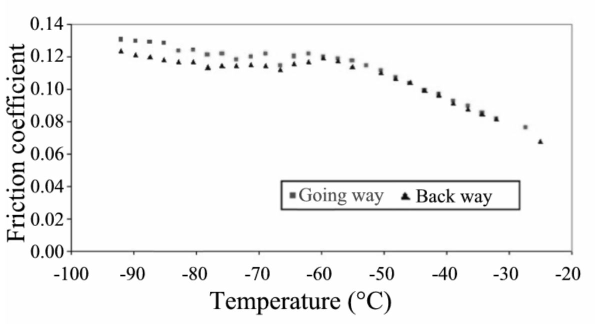

Fig. 11.: Friction coefficient against temperature under vacuum.

A dedicated test at variable temperature gives the friction coefficient evolution against the temperature as shown in the Figure 11. The friction coefficient is worst at low temperature but the graph shows clearly its improvement above -60°C. For information, this temperature corresponds to the disappearance of the stick-slip phenomenon.

C. Behavior during coil test

The measurement system was slightly different for the final test of the coil: the gauges were placed externally on the vacuum vessel and not on the posts themselves. Due to the stiffness and the form of the vacuum vessel pipe, the sensitivity was much lower than in the lab test.

The signals (Fig. 12) were very difficult to analyse. It is sure that the slide occurred but the computation of the friction coefficient is not obvious. It seems close to 0.15.

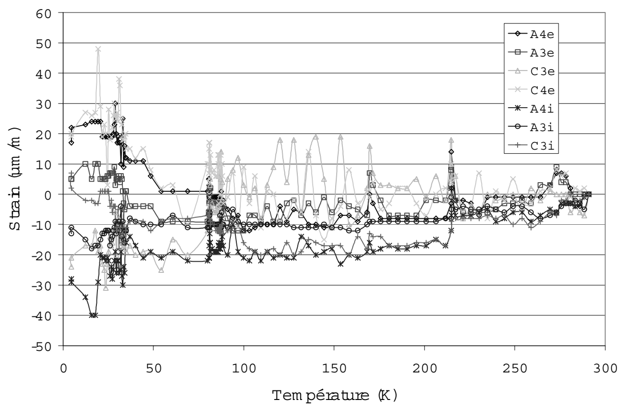

Fig. 12.: Typical graph of the gauge signals during a warm up of a coil.

IV. Conclusion

The safe design of the supports was checked by investigated tests on the real production. The measurements during the final test of the coil are relatively coherent with their expected behavior.

References

[1] P. Védrine, "Manufacturing and integration progress of the ATLAS barrel toroid magnet at CERN", in IEEE Trans. Appl. Supercond., volume 14 n°2, 2004, pp. 491-494.

[2] O. P. Anashkin, "Mechanical tests of the ATLAS Barrel Toroid tie rods", in Cryogenics, volume 45, July 2005, pp. 469-472.

[3] C. Berriaud, "On-Surface Tests of the ATLAS Barrel Toroid Coils: Acceptance Criteria and Results", MT19

[4] A. Dudarev, "On-Surface Test of the ATLAS Barrel Toroid Coils: Overview", MT19